MEASUREMENTS OF INTERACTIONS BETWEEN ACOUSTIC FIELDS AND NONUNIFORM MEAN FLOW*

K. Magiawala, J. Wat, E. Awad, F. E. C. Culick and T. Kubota

California Institute of Technology
Pasadena, California 91125

ABSTRACT

Two problems crucial to the stability of longitudinal acoustic waves in solid rocket motors are examined experimentally. The first is the dissipation of energy associated with an average flow inward at the lateral boundary. Measurements reported here, though subject to considerable experimental error, show that the actual losses are much larger than predicted by the approximate one-dimensional analysis. The second problem is the attenuation of waves accompanying reflection by the nonuniform flow in a choked exhaust nozzle. Empahsis in this work has been on technique, to provide data relatively easily and inexpensively. It appears that good results can be obtained in a routine manner using small supersonic wind tunnel operated as an open cycle. At least for Mach numbers up to 0.04 at the nozzle entrance, difficulties with signal/noise are satisfactorily overcome with a tracking filter.

INTRODUCTION

The results reported here have been obtained as part of a continuing program devoted to various problems associated with interactions between acoustic fields and non-uniform flow fields. Particular emphasis has been placed on subjects important in studies of combustion instability in tactical solid rocket motors.

Substantial contributions to the balance of acoustic energy arise with the non-uniform average flow at the lateral boundary. Approximate one-dimensional analysis (refs. 1-3) has shown that the energy loss rate per unit area is $\bar{u}_b|\hat{u}'|^2$, where $\bar{u}_b$ is the velocity inward. This constitutes a significant stabilizing influence for longitudinal waves in tactical motors. A major intent of the present program has been to determine experimentally, at room temperature, how accurately the loss is predicted by the simple analysis cited.

The method used here is an extension of earlier work (refs. 4, 5) based on a resonance tube with mean flow. In that work the influence of flow in the acoustic field near a subsonic vent was studied. According to the one-dimensional analysis, there should be a gain of energy equal to $\bar{u}_v|u'|^2$ per unit area and time. Experimental results showed the actual values to be roughly 30%

*Work supported by the Air Force Rocket Propulsion Laboratory.

larger. The same sort of apparatus but with additional pieces to provide flow inward at the lateral boundary as well as at the ends, has been used here. Again the experimental values for the energy transfer turn out to be much greater than the predicted values.

Very large experimental errors accompany these results. It appears that the only way to reduce the errors significantly - even if a different design of the apparatus is used - is to use larger equipment and as large flow rates as possible. The reason is fundamental: the interactions are small, per unit flow, and the relative errors of measurement are unavoidably large for the scale of apparatus used in this work.

The second part of this work has been concerned with the problem of measuring the admittance of a choked nozzle. By far, the most extensive previous work has been that based on a blow-down facility (refs. 6-8). In the present work we have used a continuously operating supersonic wind tunnel. Problems with noise and contamination in the flow have been solved by operating the tunnel with the circuit open. Flow enters at room temperature and pressure, passing through a long straight section terminating in the test nozzle. The straight section is used as an impedance tube. A few tests have been made with secondary flow injected at the periphery of the nozzle, up to 5% of the average flow.

To avoid using a large number of pressure gages, and to provide fine spacial resolution, a probe moveable on the axis of the impedance tube has been used to measure the pressure field. At least up to a Mach number of 0.04 in the test section a tracking filter is adequate to extract the signal from the noise at all positions in the field. It appears that the admittance can be determined routinely with an error of 5% or less.

The admittances of nozzles are in general relatively small, in particular much smaller than the values encountered in the more traditional applications of the impedance tube to measure the acoustical properties of materials. This fact has serious consequences for the procedures used in data reduction. In principle, measurements of the magnitudes and locations of maxima and minima of the pressure field are sufficient to determine the admittance function (e.g. references 9 and 10). However, it happens that in practice, this procedure is accompanied by large errors, and even ambiguities of sign, when the admittances are small.

Under those conditions, which prevail in the present work, it is essential to measure both the magnitude and phase of the pressure field and to use both pieces of information to infer the admittance function. This has not been widely recognized. A very effective procedure, described first in reference 11, has been adopted here. There is no doublt that either that or a similar technique must be used to obtain acceptable values of the admittance function for a nozzle.

MEASUREMENTS OF ACOUSTIC ENERGY LOSSES ASSOCIATED WITH INFLOW AT A LATERAL BOUNDARY

The phenomenon treated in this section has commonly come to be known as the "flow turning loss". Its existence was first established theoretically several years ago as a result of a one-dimensional analysis (references 1-3) but the data reported here constitutes the first experimental justification. Owing to constraints set chiefly by the size of the apparatus used, the results we have obtained provide only a bit more than qualitative support for the predictions.

Figure 1 is a sketch of the apparatus used. Much of the hardware is that used in earlier work (references 4 and 5) to determine the influence of the exhaust vent on acoustic waves. The new portions are the cylindrical porous tubes - the "cross flow elements" - installed as a means of introducing flow in at the lateral boundary. Thus, flow in the tube enters through both the pistons at the ends, which serve to excite acoustic waves, and through the cross flow elements. In Figure 2, the various flow and geometrical parameters are defined.

As in our earlier work, the technique centers ultimately on measurements of the resonance curve under various conditions, the width of the curve giving the value of the net loss in the system. In order to infer the flow-turning loss, it is necessary to find the difference between losses due to various contributions. That is one source of great experimental difficulty because one is forced to determine a small difference between two relatively large quantities.

A second source of difficulty has been the need to determine the admittance function for the cylindrical cross flow elements. No way has been found to make a direct measurement, and we have been forced to assume that the values measured for flat-samples are valid for the curved surfaces. Additionally, flat surfaces having the same porosity as the cylindrical surfaces are not available. It has therefore been necessary to extrapolate measured values in the following way.

Three porous plates, referred to as grades F, G and H, were obtained from the manufacturer, Pall Western Co. These were first calibrated, by measuring the variation of flow rate with pressure drop across a plate. The results, and the result for cross flow element 1 (CFE1) are shown in Figure 3; the data for element 1 are very close to those for element 2 and are omitted for clarity.

The admittance functions for the three flat samples were then measured, using an impedance tube as described in references 4 and 5. Repeated tests were made in order to determine the experimental uncertainty, as an example, the data for the real part of the admittance function for plate H are given in Table 1 and plotted in Figure 4, for the frequency equal to 445 Hz. The solid line in Figure 3 is a least squares fit to the data. Similar results were obtained for all three samples, and then plotted, as shown in Figure 5, as

the real part of the admittance versus pressure drop for several values of the average Mach number of flow through the plates.

We then make the crucial assumption that the results may be extrapolated, as indicated in Figure 3. The real part of the admittance for a cylindrical element is supposed to lie on the same line of constant Mach number (or flow speed, or flow rate) but at the value of pressure drop measured and shown in Figure 2. Table 2 is a summary of values of the real parts of the admittance functions for the two cross flow elements.

The sequence of tests required to measure the flow turning loss is the same as that used in references 4 and 5 to determine the influence of the vent, plus an additional test to encompass the contribution from the cross flow. Linear stability analysis provides the basis, the formula for the net coefficient of attenuation, α;

$$\alpha = \alpha_p + \alpha_t + \alpha_{ft} + \alpha_v + \alpha_d \qquad (1)$$

where the terms on the right hand side represent the following contributions:

α_p: attenuation constant associated with the admittance and flow for the faces of the piston drivers;

$$\alpha_p = 4f(A_p^{(r)} + \overline{M}_1) \qquad (2)$$

α_t: attenuation constant associated with the admittance and flow for the cylindrical cross-flow elements;

$$\alpha_t = 4f(A_t^{(r)} + \overline{M}_b)\, \mathcal{C}_\ell \left(\frac{S_{bs}}{S_c}\right) \qquad (3)$$

α_{ft}: attenuation constant associated with the flow turning losses, to be determined;

α_v: attenuation constant associated with the influence of the exhaust vent;

α_d: attenuation constant associated with other losses, mainly radiation and viscous losses at the lateral boundary.

With flow through both the lateral boundary and at the ends, the total flow rate through the exhaust vent is much increased above the values covered in earlier work. Only a single geometrical configuration was used, owing partly to limitations set by the air supply system, and partly because the values of α_v had not been measured at sufficiently high flow rates. The configuration was chosen to give $f = 445$ Hz, $\beta = 0.22$, $\beta_0 = 0.38$ and $S_{bs}/S_c = 4.53$; the exhaust vent had 0.5 in. diameter and the flow Mach number just downstream of the driver pistons was held constant at 4.43×10^{-4}.

Because the same hardware is used, we assume the values of

a_v and a_p reported in references 4 and 5. The values of the admittance functions for the cylindrical elements have been determined as described above, so a_t is known. Values of a_d are measured with no flow; they serve partly as a check on the validity of the techniques and results. For the present case, we found

$$a_d = a - (a_p + a_t) = 14.90 \pm 2.75 \text{ sec}^{-1} \quad . \tag{4}$$

The theoretical value for viscous and heat transfer losses calculated according to classical formulas for laminar flow is 11.20 sec^{-1}. The difference, 3.70 ± 2.75 sec^{-1} represents other contributions, probably located mainly at the driver pistions, with a small radiation loss through the lateral boundary.

Data for a_v, reported in references 4 and 5 are given in Table 3. The results obtained for a_{ft}, using equation (1), are given in Table 4 and are plotted in Figure 6. According to the one-dimensional result for the configuration treated here, the theoretical value is

$$a_{ft} = 2f\overline{M}_b \frac{S_{bs}}{S_c} \mathcal{L}_\ell \tag{5}$$

where $\mathcal{L}_\ell$ is a geometrical factor (references 2 and 3), equal to 0.97 here. Thus, a_{ft} is expected to very linear with the Mach number of flow through the boundary. The solid line in Figure 12 represents a least squares fit to the data using the equation

$$a_{ft} = \overline{a}_{ft}\big|_{\overline{M}_b=0} + \overline{M}_b\left(\frac{d\overline{a}_{ft}}{d\overline{M}_b}\right) \tag{6}$$

The derivative $da_v/d\overline{M}_b$ of equation (1) can be used with the data to provide an independent result:

$$\begin{aligned} \frac{d\overline{a}_{ft}}{d\overline{M}_b} \pm \Delta\left(\frac{da_{ft}}{d\overline{M}_b}\right) &= \frac{d\overline{a}}{d\overline{M}_b} \pm \Delta\left(\frac{da}{d\overline{M}_b}\right) \\ &\quad - 4f\left\{\frac{dA_t^{(r)}}{d\overline{M}_b} \pm \Delta\left(\frac{dA_t^{(r)}}{d\overline{M}_b}\right) + 1\right\} \\ &\quad - \left\{\left(\frac{d\overline{a}_v}{d\overline{M}}\right) \pm \Delta\left(\frac{da_v}{d\overline{M}}\right)\right\} \frac{d\overline{M}}{d\overline{M}_b} \end{aligned} \tag{7}$$

The value using the data discussed above is

$$\frac{d\overline{a}_{ft}}{d\overline{M}_b} \pm \Delta\left(\frac{da_{ft}}{d\overline{M}_b}\right) = 23000 \pm 11000 \text{ sec}^{-1} \tag{8}$$

This is a factor of 5 greater than the theoretical value 4000 sec^{-1} calculated with equation (5).

There is little doubt that there is indeed a loss of acoustic energy associated with the flow in at the lateral boundary, and that it increases with flow rate, or Mach number. Unfortunately, owing to the large experimental uncertainty associated with these results, it is not possible to state with any degree of confidence how closely the one-dimensional approximation represents the actual losses.

MEASUREMENTS OF THE ADMITTANCE FUNCTION FOR A CHOKED EXHAUST NOZZLE

Figure 7 is a sketch of the test section of the open-circuited supersonic wind tunnel. Data are reported here for the orifice shown in Figure 8 and for the adjustable nozzle with secondary flow shown in Figure 9.

All pressure measurements were taken with Bruel and Kjeier microphones. In the procedure finally adopted, a 1/2 in. microphone is mounted near the nozzle, providing a reference signal. During a test it is monitored to ensure a constant signal or, alternatively the magnitude of the pressure measured is used to normalize the pressure measured with the probe. The probe microphone is mounted in a moveable trolley; the probe itself is 1/8 in. stainless steel tubing supported at two points by 3-legged spiders.

Figure 10 is a block diagram of the instrumentation used. At lower flow speeds ($M < 0.1$) the lock-in amplifier is satisfactory for filtering the signal from the noise, but at higher speeds the tracking filter was much more effective. A single test consists of measuring the magnitude and phase of the pressure as a function of position along the tube, with the frequency and flow conditions fixed. For satisfactory results, the data must cover at least two minima of the pressure field, and the measurement locations should be more densely distributed in the vicinity of the minima. Less than two hours are required to complete a test with data taken at approximately thirty locations. Before discussing how the data is treated, it is helpful to outline analysis of the acoustic field, and the general procedure for reducing data.

For a uniform tube with uniform average flow, the stationary acoustic field may be represented as the superposition of two travelling waves. Let the nozzle be located at $z = 0$, with the test section stretching over $z > 0$. If the leftward travelling wave incident on the nozzle has amplitude a at $z = 0$, the reflected wave has complex amplitude

$$\delta = \left(\frac{1 + A}{1 - A}\right) = C|\delta|e^{i\phi}\, C$$

$$\delta = \frac{1 + A}{1 - A} = |\delta|e^{i\phi} \qquad (9)$$

$$|\delta| = \left[\frac{(1 + A_r)^2 + A_i^2}{(1 - A_r)^2 - A_i^2}\right]^{\frac{1}{2}} ; \tan \phi = \frac{-2A_i}{1 - (A_r^2 + A_i^2)} \qquad (10)$$

The admittance function of the reflecting surface is A. The pressure field may be represented as

$$p' = Ce^{-i\omega t} \left[\delta e^{(ik_+ - \kappa)z} + e^{-(ik_- - \kappa)z}\right] \qquad (11)$$

The exponentials exp(± z) represent the influence of distributed losses causing attenuation of the waves: the leftward travelling wave decays according to the factor exp (±κz).

The formula (11) represents a stationary acoustic field in which the amplitude and relative phase are functions of position along the tube. In the ideal limit of no flow, $\bar{M} = 0$, the two wave numbers k_+, k_- are equal: $k_+ = k_- = k = \omega/a$. For the case when the tube terminates with a rigid flat plate, the admittance A = 0 and (10) becomes simply

$$p' = 2Ce^{-i\omega t} \cos kz \qquad (12)$$

The amplitude is constant, equal to 2 for the normalization chosen here, and the phase changes by π radians every half wavelength from the end.

To determine k_+, k_- for the case of uniform flow, we substitute the expressions for travelling waves into the linearized acoustics equations with flow:

$$\bar{\rho} \frac{\partial u'}{\partial t} + \bar{\rho}\bar{u} \frac{\partial u}{\partial z} + \frac{\partial p'}{\partial z} = \mp Gu' \qquad (13)$$

$$\frac{\partial p'}{\partial t} + \bar{u} \frac{\partial p'}{\partial z} + \bar{\rho} \frac{\partial u}{\partial z} = 0 \qquad (14)$$

Distributed losses are represented by the term $\mp Gu'$, the upper sign for a rightward travelling wave. Now set

$$p' = P_{\pm} e^{-i\omega t} e^{\pm(ik_\pm - \kappa) z} \qquad (15)a,b$$

$$u' = U_{\pm} e^{-i\omega t} e^{\pm(ik_\pm - \kappa)z}$$

and substitute into (12) and (13). The condition for non-trivial

solutions $P_{\pm}$, $v_{\pm}$ leads eventually to the results

$$k_{+} = \frac{k}{1+\bar{M}} \qquad k_{-} = \frac{k}{1-\bar{M}} \tag{16}$$

$$\kappa = \tfrac{1}{2}\left(\frac{1-\bar{M}}{1+\bar{M}}\right)\frac{G}{\rho_o a_o} \tag{17}$$

The second equation relates κ and G, and is used in later processing of data. With the formulas (16), equation (11) may be put in the form

$$p' = C\left[\delta e^{iKz} + e^{-iKz}\right] e^{-i(\omega t+\bar{M}\, z)} \tag{18}$$

with $K = k + i\kappa$. This may be re-written to show the amplitude and phase explicitly. For example, if distributed losses are ignored, $\kappa = 0$, $K = k$ and (18) can eventually be written

$$p' = CPe^{-i(\omega t + \bar{M}Kz - \psi_p)} \tag{19}$$

where

$$P = 1 + |\delta|^2 + 2|\delta| \cos\,(2Kz + \phi) \tag{20}$$

$$\tan \psi_p = \frac{-\sin\ z + |\delta| \sin\,(Kz + \phi)}{\cos\ z + |\delta| \cos\,(Kz + \phi)} \tag{21}$$

A similar but more complicated form of (19) can be written for $\kappa \neq 0$. The point is that both the amplitude, P, and the phase, $\bar{M}Kz - \psi p$, are strong functions of position, depending on the admittance of the end surface, the flow Mach number and the distributed losses.

An alternative form sometimes used is

$$p' = -2Ce^{\pi\alpha_o + i(\pi\beta_o + \bar{M}Kz)} \sinh \pi(\alpha+i\beta) \tag{22}$$

where by definition, the quantity δ introduced above is written

$$\delta = -e^{2\psi};\ \psi = \pi\,(\alpha_o + i\beta_o) \tag{23}$$

and

$$\alpha = \alpha_o - \frac{\kappa z}{\pi} \; ; \; \beta = \beta_o + \frac{Kz}{\pi} \qquad (24)a,b$$

The distributed losses are now accounted for.

In most uses of the impedance tube, as for example in references 9 and 10, only the amplitude of the pressure distribution has been measured. The real and imaginary parts of the admittance function are then determined by fitting data to the function P, equation (20), or to the corresponding formula deduced from (22):

$$|p'| = 2Ce^{\pi\alpha_o} \left[\cosh^2 \pi(\alpha_o - \frac{\kappa z}{\pi}) - \cos^2\pi(\beta_o + \frac{Kz}{\pi})\right]^{\frac{1}{2}} \qquad (25)$$

The formula for the phase is

$$\phi = \pi\beta_o + \bar{M}Kz + \tan^{-1}\left[\coth \pi(\alpha_o - \frac{\kappa z}{\pi}) \tan \pi(\beta_o + \frac{Kz}{\pi})\right] \qquad (26)$$

We had anticipated that the traditional technique based on amplitude only, should work satisfactorily in the application we envisaged. After considerable effort had been expended, we established beyond question that if the admittance function is relatively small, as the case is for nozzles, then the technique is extraordinarily sensitive to small errors in the data and is useless in practice. It is essential that measurement be taken of both the amplitude and phase distributions, and that both quantities be used, with suitable analysis of the acoustic field, to deduce the admittance function and distributed losses.

As a simple example illustrating one reason that the method is ineffective, consider the case defined by C = 200, β = 0.57, κ = 0.0306. Figure 10 shows the pressure amplitude for α_o = -0.01 (solid line) and a few points for α_o = +0.01, all computed with equation (25). The results for the two values of α_o are indistinguishable except in the immediate vicinity of the minima. These are reasonable values for the parameters, with $\alpha_o > 0$ corresponding to a positive real part for the admittance. This shows that in practice, with the sorts of experimental uncertainties one must expect, the technique will not even determine the sign of the real part of the admittance - which governs the gain or loss of energy at the surface. The reason why this happens is easily seen from equation (25) with κ = 0. The term $\cosh^2\pi\alpha_o$ is insensitive to the sign of α_o, and when α_o is small, only a small change of the parameter C is required to produce the same pressure distribution for α_o positive or negative, i.e. to provide the required value of C exp ($\pi\alpha_o$).

We have used both the Newton-Raphson method, and a non-linear regression technique with equations (25) and (26), but a technique developed by Baum, reference 11, appears to be the most efficient way to process the data. This is based on formal integration of the linearized equations (13) and (14), subject to the boundary condition specified in terms of the admittance function. In the case when G is constant, this is entirely equivalent to using the closed form solutions (18) or (22). All of the results described below have been obtained using that method (reference

11) which is relatively straightforward and inexpensive to use, and provides high accuracy.

The procedure has been checked quite thoroughly for idealized problems. Values for the admittance are specified, and the exact pressure and velocity fields calculated using equations (13) and (14). The results are used as "data" and Baum's method used to compute the admittance and the distributed losses. Errors less than one part in 10^6 arise in all cases; these can be reduced by increasing the precision of the numerical calculations.

A few examples have been worked out with a random error distribution superposed on the theoretical data. For errors up to ± 3.5% of the maximum pressure amplitude applied to all data points (i.e. in the vicinity of minima as well as maxima) the errors in the admittance function are less than 6%; there is essentially no change in the values of G, or κ, inferred.

Figure 12 shows results found for an orifice nozzle (Fig. 8) operating with upstream Mach number equal to 0.04. For a short nozzle, the admittance function is $(\alpha - 1)\bar{M}_e/2$ where $\bar{M}_e$ is the Mach number at the entrance. For $\bar{M}_e = 0.04$, the value is 0.008. If the convective influence of the mean is included as part of the boundary condition, the net result is $(\alpha + 1)\bar{M}_e/2$ which equals 0.048, very close to the values shown in Figure 12. This suggests that, owing to the large separation/recirculation zones in the corner at the end of the tube, the admittance measured really is that for an effective nozzle with diameter equal to the tube diameter. This matter will be discussed further in subsequent work.

The more interesting influence of secondary flow is shown in Figure 13 There seems to be little influence until the frequency is above 1000 Hz., for the nozzle tested here. At 2000 Hz., the secondary flow evidently contributes a very substantial net gain, a result which has not previously been reported.

For the data reported here, the experimental errors are roughly 5%. Further results will be reported later.

REFERENCES

1. Culick, F. E. C., "The Stability of One-Dimensional Motions in a Rocket Motor," Combustion Science and Technology V. 7 (1973) pp. 165-175.

2. _____ "Linear Analysis of One-Dimensional Oscillations in a Variable-Area T-Burner," 9th JANNAF Combustion Meeting (1972).

3. "T-Burner Testing of Metallized Solid Propellants," (F.E.C. Culick, Ed.) AFRPL-TR-74-28 (1974), C.P.I.A. Publication 275 (March 1976).

4. Magiawala, K. and Culick, F.E.C., "Measurements of Energy Losses Associated with Interactions Between Acoustic Waves and a Steady Flow Field," AFRPL-TR-78-6 (March 1978).

5. _____ "Measurements of Energy Exchange Between Acoustic Fields and Non-Uniform Steady Flow Fields," J. Vibration and Sound (to be published).

6. Zinn, B. T., Daniel, B. R., Janardan, B. A., and Smith, A. J., Jr., "Damping of Axial Instabilities by the Minuteman II, Stage III, and Minuteman III, Stage III, Exhaust Nozzles," AFRPL-TR-72-71 (August 1972).

7. _____ "Nozzle Design Considerations for Attenuation of Axial Instabilities in the Minuteman II and III, Stage III Rocket Motors," AFRPL-TR-73-69 (September 1973).

8. Bell, W. A., Daniel, B. R., and Zinn, B. T., "Experimental and Theoretical Determination of the Admittances of a Family of Nozzles Subjected to Axial Instabilities," J. Vibration and Sound, V. 30, No. 2 (1973) pp. 179-190.

9. Morse, P. M., Vibration and Sound,McGraw-Hill Book Co., New York (1935).

10. Tippert, W. K. R., "The Practical Representation of Standing Waves in an Acoustic Impedance Tube," Acustica, V. 3 (1953), pp. 153-160.

11. Baum, J., Daniel, B. R., and Zinn, B. T., "Determination of Solid Propellant Admittances by the Impedance Tube Method," AIAA 18th Aerospace Sciences Meeting (January 1980) AIAA Paper No. 80-028).

TABLE 1

Data for the admittance of a Porous Plate, grade PSS 'H', f = 445 Hz.

$\overline{M}_b \times 10^4$	$A_b^{(r)} \times 10^2$	$\overline{A}_b^{(r)} \times 10^2$	$\sigma \times 10^6$
0	1.250 1.266 1.206	1.241	252
0.97	1.234 1.234 1.243	1.237	40
1.95	1.397 1.391 1.370	1.386	114
2.92	1.328 1.366 1.137	1.354	180
3.90	1.444 1.440 1.429	1.438	63
4.87	1.437 1.492 1.458	1.462	225

TABLE 2

Averaged Admittance Functions for the Two Cross Flow Elements at 445 Hz

$\overline{M}_b \times 10^4$	$\overline{A}_b^{(r)} \times 10^2$	$\sigma \times 10^6$
0	0.5320	599
0.97	0.3862	1335
1.05	0.4512	228
2.92	0.4307	196
3.90	0.4576	172

TABLE 3

Values of the Average Attenuation Coefficient and Standard Deviation for a Circular Vent, $\frac{1}{2}$" diameter, at 442.7 Hz (refs. 4 and 5).

$\overline{M} \times 10^4$	$\bar{a}_v$ (sec^{-1})	Δa_v (sec^{-1})
0	0.06	0.70
4.43	-0.59	0.85
8.86	-0.90	0.78
13.29	-1.15	0.72
17.72	-2.39	1.00
22.15	-3.15	0.73

TABLE 4

Values of the Average Attenuation Coefficient and Standard Deviation for Flow turning losses, at 445 Hz.

$\overline{M}_b \times 10^4$	$\bar{a}_{ft}$(sec^{-1})	Δa_{ft}(sec^{-1})
0	-0.33	6.42
0.97	+7.23	9.48
1.95	+5.04	4.95
2.92	+6.75	5.01
3.90	+6.42	4.64

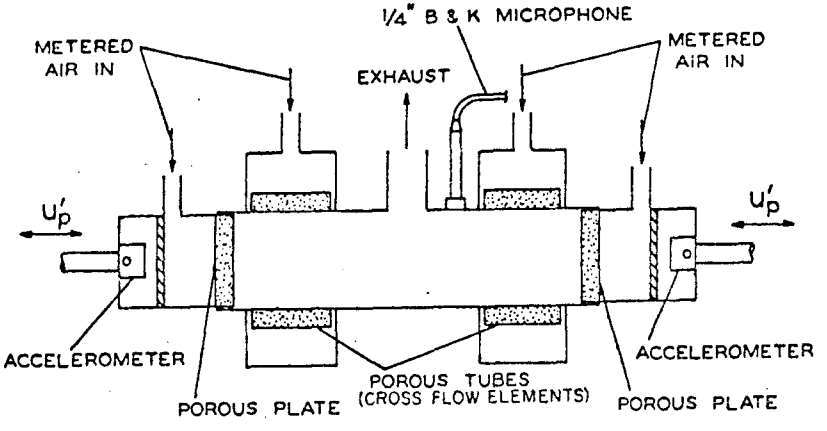

Figure 1.

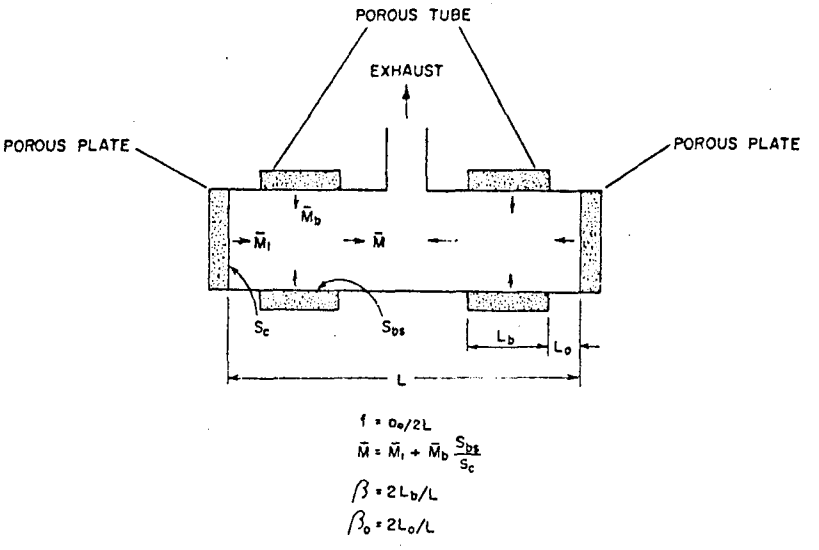

Figure 2.

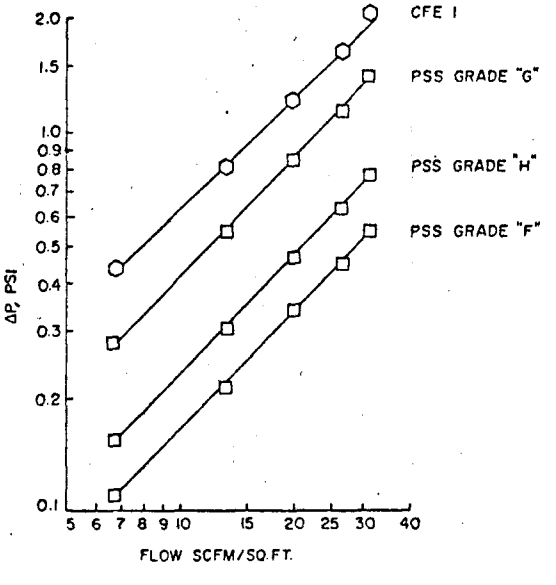

Figure 3.

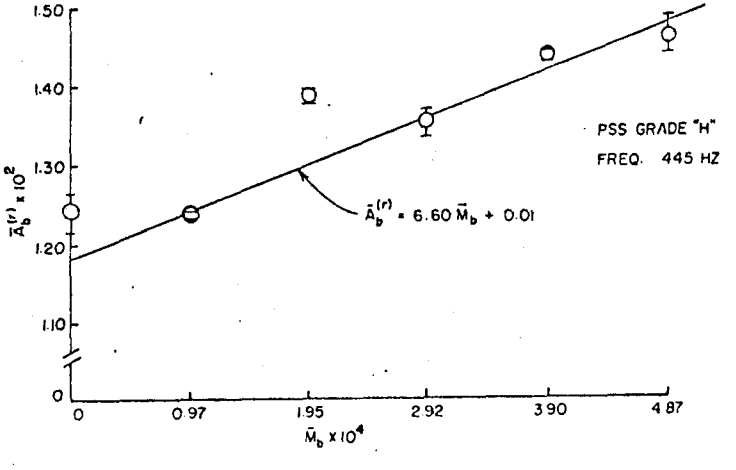

Figure 4.

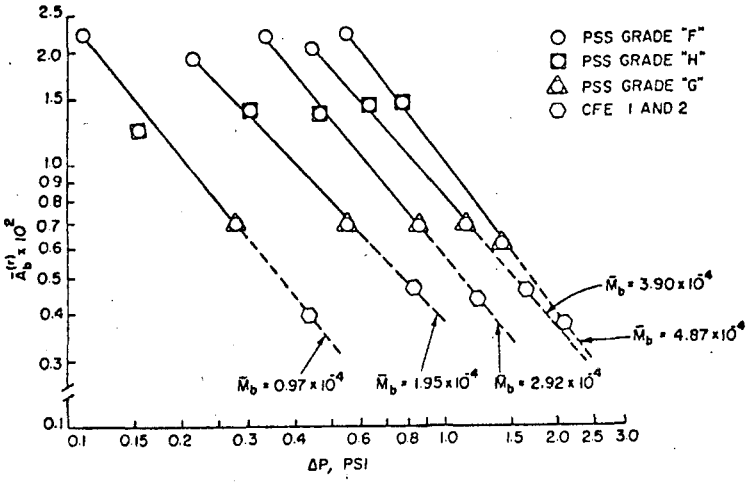

Figure 5.

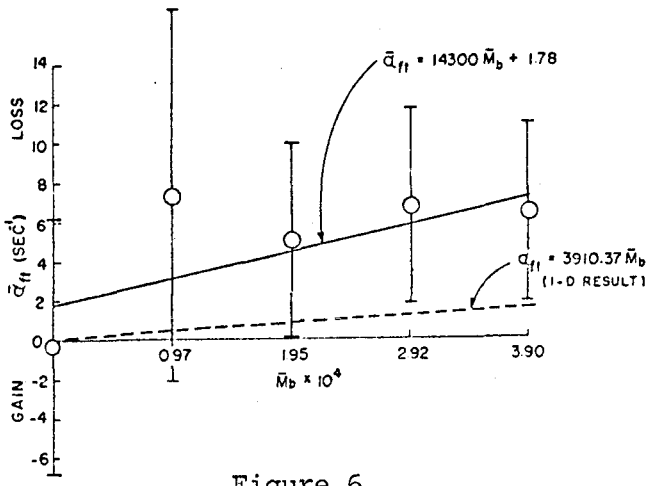

Figure 6.

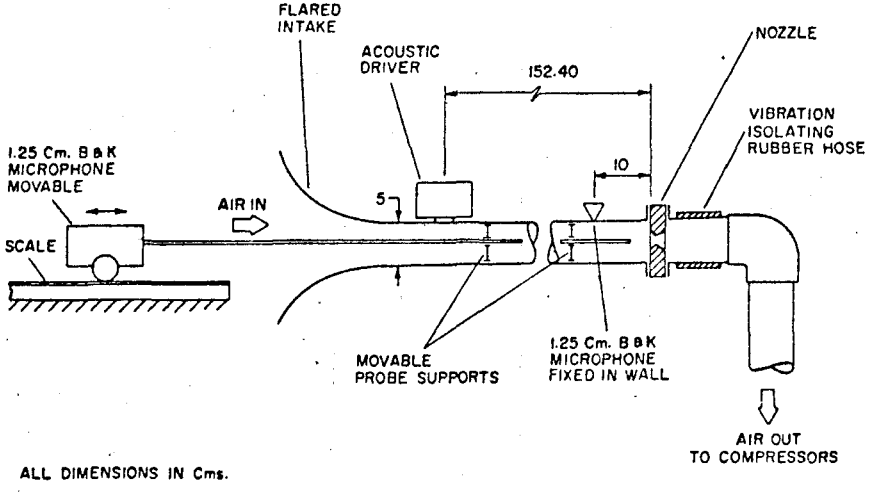

Figure 7.

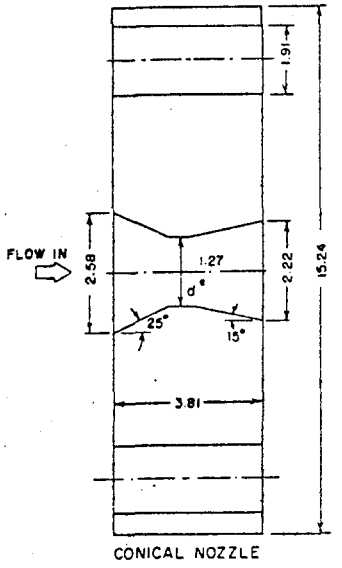

Figure 8.

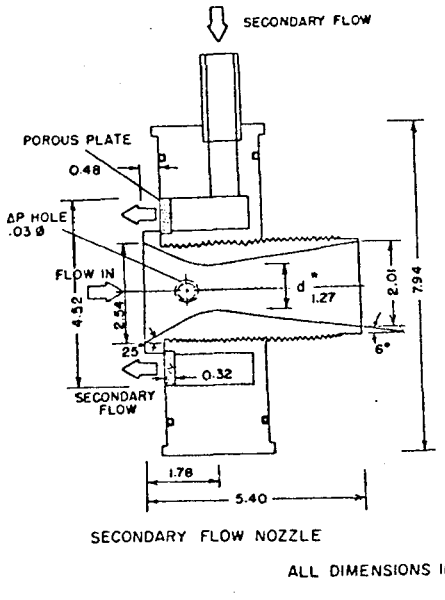

Figure 9.

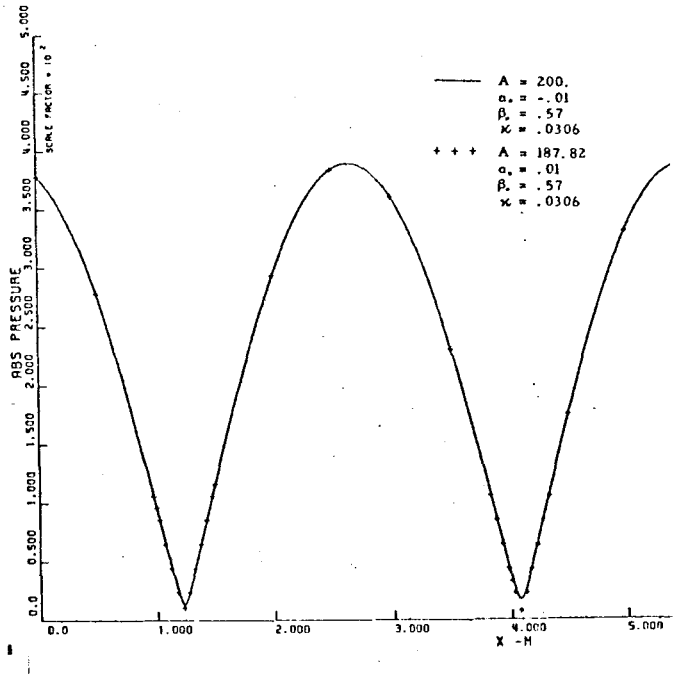

Figure 11.

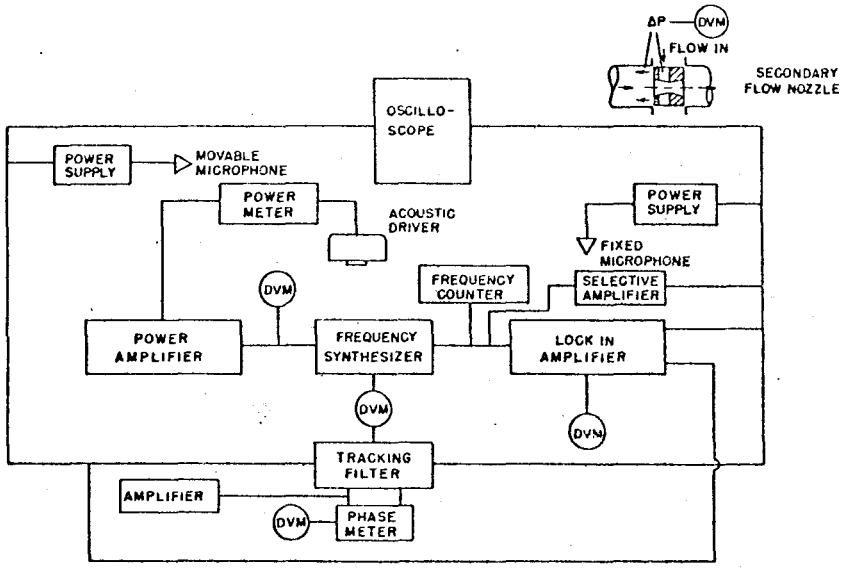

Figure 10.

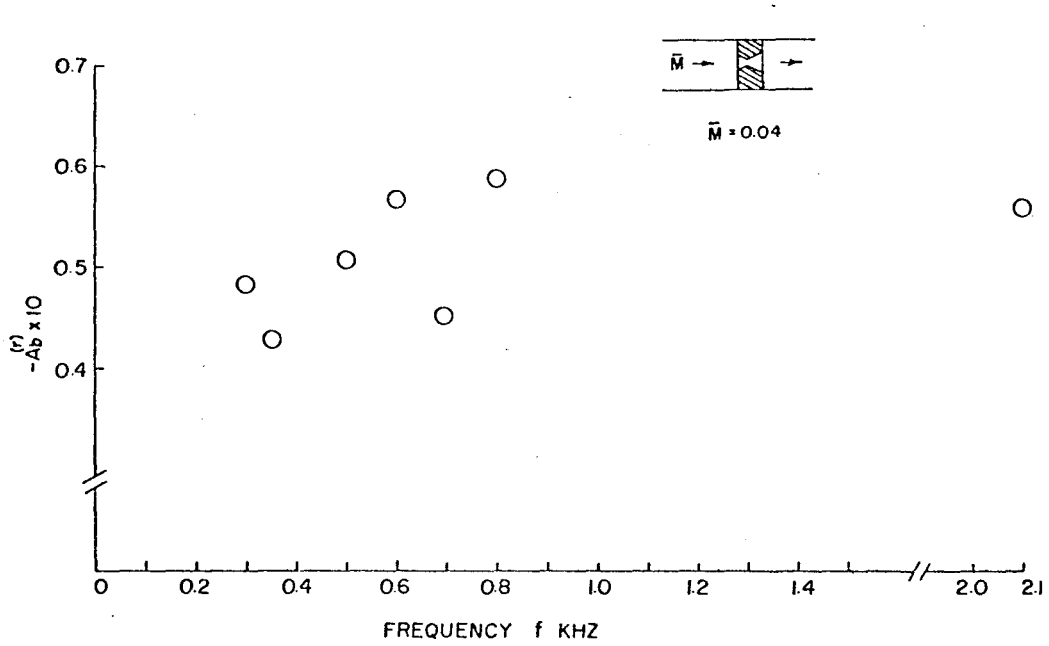

Figure 12.

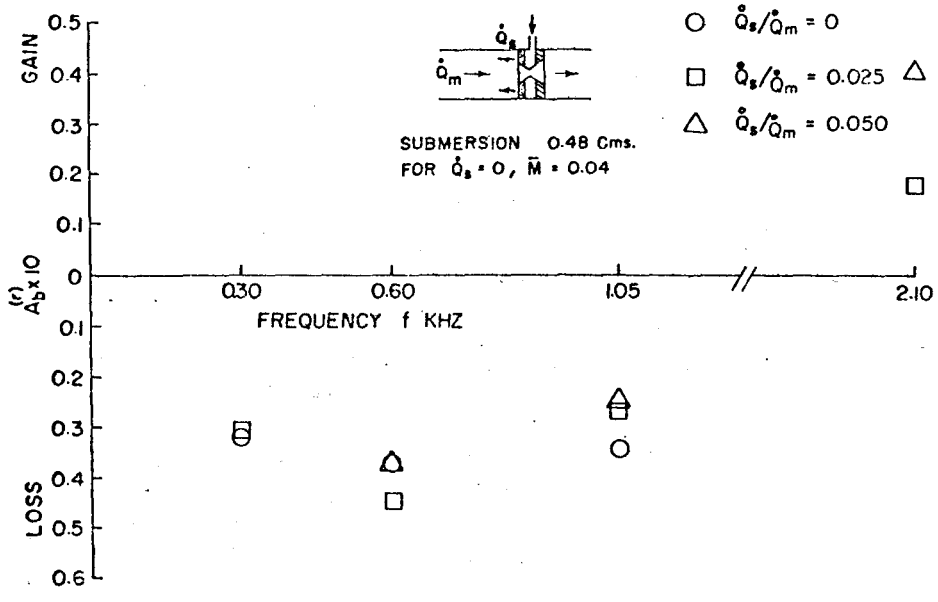

Figure 13.